Journal of Materials Chemistry A

PAPER

View Article Online
View Journal | View Issue

Cite this: J. Mater. Chem. A, 2014, 2, 3971

Palladium nanoparticles encapsulated in magnetically separable polymeric nanoreactors†

Ester Weiss, Bishnu Dutta, Yafit Schnell and Raed Abu-Reziq*

Received 2nd December 2013
Accepted 6th January 2014

DOI: 10.1039/c3ta14992g

www.rsc.org/MaterialsA

A method for immobilization of palladium nanoparticles in magnetically separable polymeric nanocapsules is presented. The method is based on co-encapsulation of palladium nanoparticles stabilized by hyperbranched polyamidoamine (H-PAMAM-C_{15}) modified with palmitoyl groups and hydrophobic magnetite nanoparticles within polyurea nanospheres. The synthesis of these polyurea nanospheres is based on nanoemulsification of chloroform, containing magnetic nanoparticles and palladium acetate, in water using suitable surfactants or dispersants. Then, the chloroform nano-droplets are confined in a polyurea shell formed by interfacial polycondensation between isocyanate and amine monomers. The palladium acetate was reduced with hydrogen to create palladium nanoparticles dispersed in the core of the polyurea nanocapsules. These catalytic polymeric nanoreactors were utilized in hydrogenation of alkenes and alkynes in water. The nanoreactors were easily separated from the reaction mixture *via* application of external magnetic field. The recyclability of these nanoreactors was examined in hydrogenation of styrene; no significant change was observed in their reactivity for up to four cycles.

Introduction

In the past decades catalysis by metal nanoparticles (NPs) has been intensively investigated due to their large surface area and unique properties.[1] The nanoparticles have two major drawbacks; they tend to aggregate and their recovery using trivial procedures is difficult. Employing an electrostatic, steric or electrostatic–steric stabilizer can prevent aggregation of metal nanoparticles. Common stabilizers are organic polymers,[2] dendrimers,[3] surfactants[4] and organic ligands.[5] Recoverability is achieved by immobilization of NPs that also can prevent their aggregation. Immobilization on solid supports,[6] such as inorganic materials and organic polymers, is used extensively. Other immobilization techniques are based on encapsulation of metallic NPs in sol–gel matrices[7] and in metal organic frameworks.[8] In addition, encapsulation of metal NPs in the shell of polymeric microcapsules has attracted a great deal of attention in the past years, because it provides immobilization and protection of NPs from the reaction media.[9] For example, encapsulation of palladium nanoparticles and their application in catalytic hydrodechlorination of chlorophenols were demonstrated.[10] The separation and the recyclability of these encapsulated catalysts were easily enabled by centrifugation.

Magnetic nanoparticles (MNPs) have been recently utilized widely as supports for catalysts, by modification of the MNP surface.[11] The supported catalysts have proven to be effective in numerous organic transformations and were easily separated from the reaction media by applying an external magnetic field. Magnetic nanoparticles have also been utilized recently in immobilization of metal nanoparticles.[12] These magnetically separable metal nanoparticles are prepared mainly by adsorption of metal ions on the surface of the magnetic nanoparticles. This can be done by using functionalized MNPs with coordinating groups or using MNPs coated with a silica layer, containing specific stabilizing groups. Finally, the loaded ions are reduced with hydrogen, sodium borohydride or hydrazine.

Here, we present a new method for the immobilization of palladium nanoparticles that can be magnetically separable as well. The method is based on encapsulation of palladium nanoparticles and hydrophobic MNPs in the core of polyurea nanocapsules. These nanocapsules were prepared by nanoemulsification and interfacial polymerization between isocyanate and amine monomers.[13] The resulted new materials were characterized and their catalytic activity was explored in hydrogenation of alkenes and alkynes in aqueous medium. By applying an external magnetic field, they were easily separated from the reaction medium and were recycled four times in hydrogenation of styrene in water.

Institute of Chemistry, Casali Center of Applied Chemistry and the Center for Nanoscience and Nanotechnology, The Hebrew University of Jerusalem, Jerusalem 91904, Israel. E-mail: Raed.Abu-Reziq@mail.huji.ac.il; Fax: +972-4-6585469; Tel: +972-2-6586097

† Electronic supplementary information (ESI) available: SEM images and DLS measurements of polyurea nanocapsules formed from different amine and isocyanate monomers, EDS analysis of MNPs@PU capsules, and the TGA curve of Pd_{nano}/MNPs@PU. See DOI: 10.1039/c3ta14992g

Results and discussion

Synthesis and characterization of polyurea nanocapsules

Generally, the polyurea nanocapsules were prepared in two steps. The first step included nanoemulsification of chloroform, containing the isocyanate monomer, in water. Stabilization of the chloroform nano-droplets in water was performed using 4% of surfactant. In the second step, interfacial polycondensation reaction occurred when an amine monomer was added slowly to the chloroform–water nanoemulsion. Polymeric nanospheres were formed after stirring for 16 hours at room temperature. The preparation process is illustrated in Scheme 1. To optimize the synthesis process of the polyurea nanocapsules, different parameters such as the type of the surfactant, the isocyanate and the amine monomers, were examined and their effect on the polymeric nanocapsule structure was studied.

Initially, different surfactants were employed in the preparation of nanocapsules. The monomers polymethylene polyphenyl isocyanate (PAPI 27) and 1,6-hexamethylenediamine (HMDA) were selected to create the polyurea shells. In particular, the polyoxyethylene (20) sorbitan monooleate (Tween 80), polyoxyethylene (20) stearyl ether (Brij 78), butylated polyvinylpyrrolidone (Bu-PVP), sodium dodecyl sulfate (SDS), cetyltrimethylammonium chloride (CTAC) and the dispersant lignosulfonic acid (Reax 88A) were tested. Phase separation was observed during the interfacial polymerization when Brij 78 was utilized to stabilize the nanoemulsion. When Tween 80 was used, only polyurea chunks were produced. All other surfactants enabled formation of polyurea capsules. However, the desired small-sized polyurea nanocapsules could be obtained only when the surfactant CTAC or the dispersant Reax 88A was utilized. This was indicated by dynamic light scattering (DLS) measurements (Table 1) and scanning electron microscopy (SEM) images (Fig. 1). In addition, transmission electron microscopy (TEM) analysis (Fig. 2) showed a core–shell structure indicating the formation of hollow nanocapsules.

The effect of the amine and isocyanate monomers on the construction of polyurea nanocapsules was examined with Reax 88A as the stabilizer of the nanoemulsions. The monomers used were HMDA and diethylenetriamine (DETA), as the amine monomers, and 4,4′-metyhlene-bis(cyclohexylisocyanate) (MBDI), 2,4-toluene diisocyanate (TDI), 1,6-hexamethylene diisocyanate (HDI) and PAPI 27, as the isocyanate monomers. SEM images (ESI, Fig. S1†) and DLS measurements (ESI, Table S1†) indicate that nanocapsules were produced when the combinations of PAPI 27 and DETA or HMDA, as well as the combination of MBDI and DETA or HMDA, were used. In the presence of PAPI 27 the capsules formed were smaller; therefore, the isocyanate PAPI 27 was chosen as the optimized isocyanate monomer. The monomers PAPI 27 and DETA are trifunctional monomers, and in their presence highly cross-linked shells can be formed. The degree of cross-linking affects the diffusion of the substrate into the capsule core. Thus, in order to form strong shells that enable diffusion of the reactants into the nanocapsules, HMDA and PAPI 27 were chosen as the monomers for building the polymeric shells.

The effect of the PAPI 27 : HMDA molar ratios on the formation of polyurea nanocapsules was examined using seven different molar ratios: 1 : 0.4, 1 : 0.7, 1 : 0.9, 1 : 1.1, 1 : 1.25, 1 : 1.5 and 1 : 1.73, using Reax 88A as the emulsion stabilizer. SEM images (ESI, Fig. S2†) and DLS measurement (ESI, Table S2†) showed no significant change in the nanocapsule size. Furthermore, Brunauer–Emmett–Teller (BET) measurements were performed for both PAPI 27 : HMDA molar ratios, 1 : 1 and 1 : 1.73; the pore radius observed was 24.636 Å and 33.028 Å, respectively.

Table 1 Average size distribution of capsules formed using different surfactants or dispersants

Entry	Surfactant	Average size distribution (nm)
1	Bu-PVP	1755
2	SDS	245
3	CTAC	114
4	Tween 80	Polyurea chunks
5	Reax 88	105

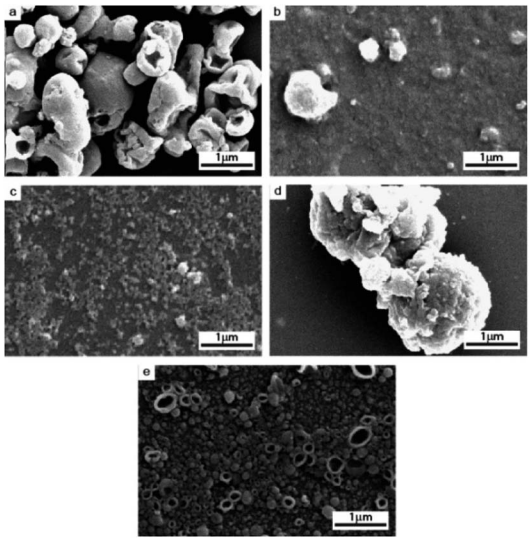

Fig. 1 SEM images of polyurea nanocapsules obtained using the following surfactants and dispersants: (a) Bu-PVP, (b) SDS, (c) CTAC (d) Tween 80 and (e) Reax 88A.

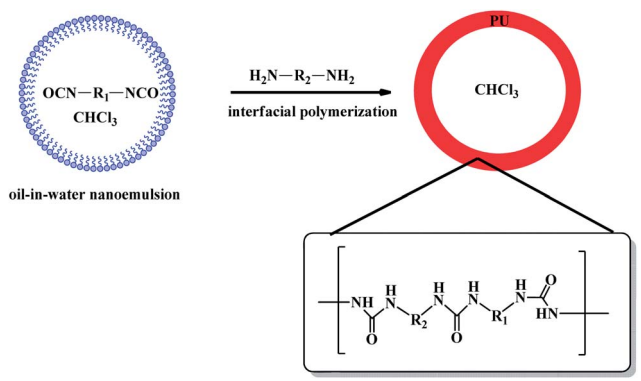

Scheme 1 Preparation of polyurea nanocapsules.

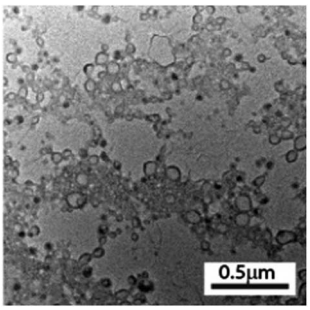

Fig. 2 TEM images of polyurea nanocapsules obtained using Reax 88A, with an isocyanate amine molar ratio of 1 : 1.73.

Magnetically separable polyurea nanocapsules (MNPs@PU nanocapsules)

Encapsulation of MNPs in polyurea nanocapsules was performed using a similar procedure utilized in the preparation of polyurea nanospheres. Therefore, chloroform containing magnetite nanoparticles coated with oleate groups and PAPI 27 was nanoemulsified in water. HMDA was added in order to start interfacial polymerization, thus yielding magnetically separable polyurea nanocapsules. This process was studied using two different PAPI 27 : HMDA molar ratios, 1 : 1 and 1 : 1.73, in the presence of CTAC or Reax 88A as the stabilizer. Both molar ratios enabled the formation of nanocapsules. According to DLS measurements, when 1 : 1 molar ratio was applied the average size of the nanocapsules was 106 nm and 110 nm in the presence of CTAC and Reax 88A, respectively. At 1 : 1.73 ratio, capsules were formed with an average size of 113 nm and 224 nm using CTAC and Reax 88A, respectively. Although when CTAC was used with 1 : 1 molar ratio, TEM analysis indicated that the MNPs were not encapsulated (Fig. 3a and b). A shell–core structure was observed, indicating that polyurea nanocapsules were formed though no MNPs were found within the core (Fig. 3a). MNPs were only seen outside the capsule (Fig. 3b). At 1 : 1.73 ratio, encapsulation of MNPs was partially achieved and MNPs were seen outside the capsules as well as within; as observed in TEM images (Fig. 3c). It seems that the MNPs were extracted from the oil droplets during the formation process of the nanocapsules. This may be explained by the ability of CTAC to form micelles in water, which can extract the MNPs and stabilize them in the aqueous medium.

In the presence of the dispersant Reax 88A at 1 : 1 isocyanate : amine ratio, the MNP encapsulation was accomplished, although most of the capsules observed by TEM were empty (Fig. 4a). Furthermore, a small fraction of non-encapsulated MNPs was observed (Fig. 4b). On the other hand, the encapsulation process of MNPs at 1 : 1.73 isocyanate : amine ratio was successful, and no MNPs were seen outside the nanocapsules (Fig. 4c). Energy dispersive X-ray spectroscopy (EDX) measurement (ESI, Fig. S3†) was performed and coincided with TEM analysis, which demonstrated encapsulation of MNPs, within the polymeric nanocapsules. In addition, X-ray diffraction (XRD) measurements were performed (ESI, Fig. S4†). The XRD pattern shows characteristic peaks of magnetite, Fe_3O_4.

The encapsulation of MNPs within the core enables facile separation of the nanocapsules from the aqueous medium, by applying an external magnetic field. In order to ensure fast and easy separation different loading percentages of MNPs were examined. In all loading percentages polyurea nanocapsules were formed. Though, at low loading percentages, 1.5%, TEM analysis (Fig. 5a) revealed that the nanocapsules formed are mostly empty capsules. With loading percentages of 2.5% and above, TEM images (Fig. 5) indicate that the nanocapsules formed contain the required MNPs. In order to facilitate fast separation of the polyurea nanocapsules, the loading percentage was chosen to be 9%.

Palladium nanoparticles encapsulated in polyurea nanoreactors (Pd_{nano}@PU nanocapsules)

After establishing a method for the formation of magnetically separable nanocapsules, their ability to act as nanoreactors was

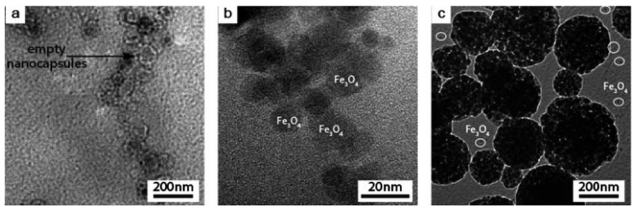

Fig. 3 TEM images of MNPs@PU nanocapsules prepared in the presence of CTAC with different amine : isocyanate molar ratios. (a and b) Ratio of 1 : 1; (c) ratio of 1 : 1.73.

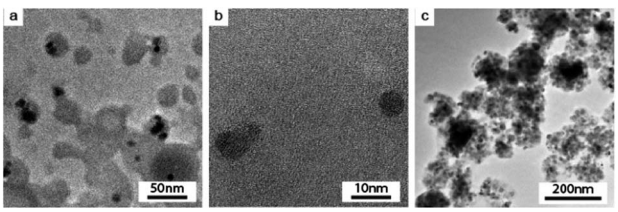

Fig. 4 TEM images of MNPs@PU nanocapsules prepared in the presence of Reax 88A with different amine : isocyanate molar ratios. (a and b) Ratio of 1 : 1; (c), ratio of 1 : 1.73.

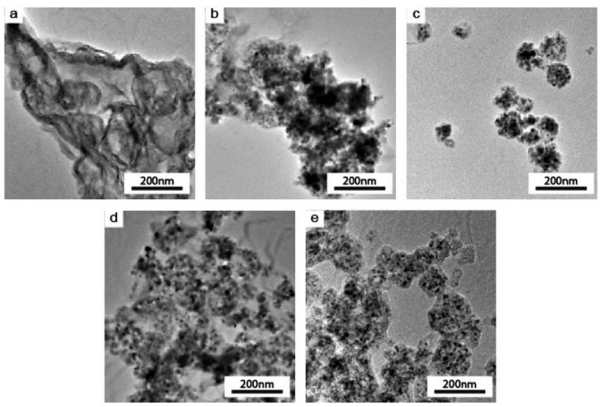

Fig. 5 TEM images representing different MNP loading percentages. (a) 1.5%, (b) 2.5%, (c) 5%, (d) 7.5% and (e) 9%.

examined. Thus, palladium acetate and hyperbranched polyamidoamine modified with palmitoyl groups (H-PAMAM-C_{15}) (Scheme 2) were dissolved in chloroform and nanoemulsified in water. This was followed by polycondensation to form polyurea nanocapsules. The resulting nanocapsules were treated with hydrogen in order to reduce Pd(II) to Pd(0), and the Pd_{nano}@PU catalyst was obtained. In order to prevent aggregation of the formed Pd nanoparticles, H-PAMAM-C_{15} was added. H-PAMAM-C_{15} can stabilize Pd particles *via* coordinative interaction between the amine groups of the H-PAMAM-C_{15} and Pd nanoparticles.

SEM analysis (Fig. 6a) of the resultant heterogeneous catalyst revealed aggregates with apparent border lines between each nanocapsule, indicating that the aggregation is due to the high vacuum required for imaging. This correlates with the average size distribution obtained in DLS measurements. DLS measurements showed an average size of 220 nm, an increase of 100 nm in the capsules size (ESI, Table S3,† Entry 1 and Entry 2), after encapsulation of the palladium nanoparticles. Apparently, encapsulation of H-PAMAM-C_{15} and palladium acetate, which was converted to palladium nanoparticles, within the nanocapsules, led to the increase in their size. TEM analysis (Fig. 6b) indicates that palladium nanoparticles are formed and encapsulated within the polyurea nanocapsule. The average size of the palladium nanoparticles was 10.3 nm (ESI, Fig. S5†).

Palladium nanoparticles encapsulated in magnetically separable nano-reactors (Pd_{nano}/MNPs@PU nanocapsules)

After achieving the ability of polyurea nanocapsules to be easily separated, by encapsulation of MPNs, as well as to perform as heterogeneous catalysts, by encapsulation of palladium acetate and their reduction, our goal was to combine both abilities and form recyclable catalytic nanoreactors. Therefore, MNPs, palladium acetate, H-PAMAM-C_{15} and PAPI 27 were dissolved in chloroform and nanoemulsified in water. This was followed by the addition of HMDA, to form a polyurea nanocapsule by interfacial polymerization. The resulting nanocapsules were treated with hydrogen, in order to form the desired heterogeneous catalyst Pd_{nano}/MNPs@PU. The preparation process is illustrated in Scheme 3.

SEM and TEM analyses (Fig. 7) reveal formation of polyurea nanocapsules, with an average size of 220 nm correlating with data obtained using DLS (ESI, Table S3,† Entry 3). EDX measurements show the presence of Pd and Fe, demonstrating that simultaneous encapsulation of Pd and MNPs was achieved (Fig. 8). Further indication for the presence of Pd in the nanocapsules was obtained using inductively coupled plasma (ICP) mass spectrometry measurements, in which the Pd concentration was 0.013 mmol g^{-1}. In addition, thermal gravimetric analysis (TGA) measurements (ESI, Fig. S6†) show that the nanocapsules are composed of 9% non-decomposable materials attributed to the MNPs and the Pd nanoparticles. Furthermore, the TGA curve demonstrates a total weight loss of 5% at 50 °C, ascribed to the removal of volatile compounds, such as chloroform. The sharp mass reduction step at 220 °C (86%) corresponds to the decomposition of the polyurea shell and H-PAMAM-C_{15}.

Catalytic application of Pd_{nano}/MNPs@PU nanocapsules

The catalytic ability of the magnetically separable catalyst Pd_{nano}/MNPs@PU was examined in hydrogenation reaction of

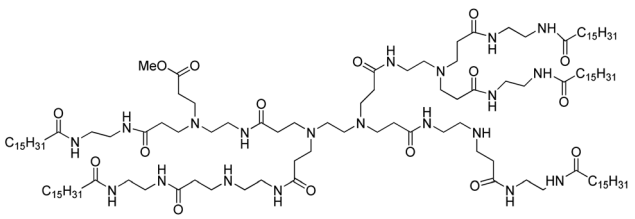

Scheme 2 Structure of hyperbranched polyamidoamine modified with palmitoyl groups (H-PAMAM-C_{15}).

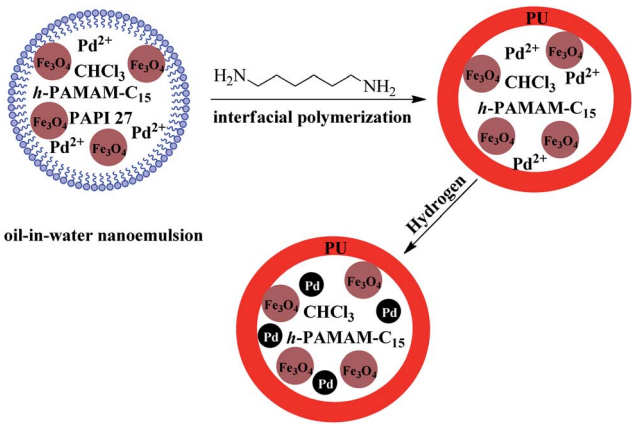

Scheme 3 Preparation of Pd_{nano}/MNPs@PU nanocapsules.

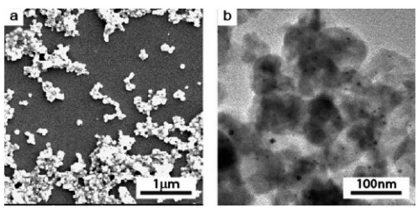

Fig. 6 (a) SEM image of Pd_{nano}@PU nanocapsules after treatment with hydrogen. (b)TEM image of Pd_{nano}@U nanocapsules after treatment with hydrogen.

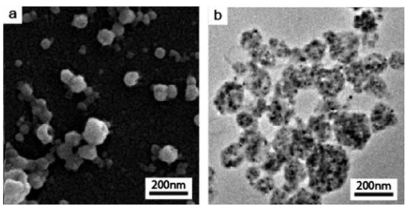

Fig. 7 (a) SEM image of Pd_{nano}/MNPs@PU nanoreactors. (b)TEM image of Pd_{nano}/MNPs@PU nanoreactors.

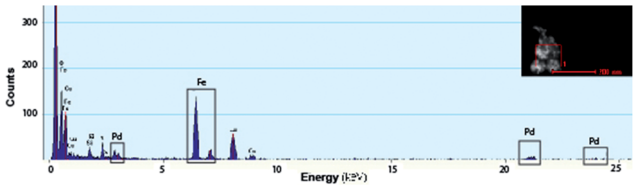

Fig. 8 EDX measurement of Pd_{nano}/MNPs@PU nanoreactors.

various alkenes and alkynes, in aqueous media. The reactions were performed under 200 psi of hydrogen for 6.5 hours. After the reactions complete, the catalyst was easily separated from the reaction medium *via* an external magnetic field. These results are summarized in Table 2.

The reduction of aromatic alkenes was successful, and saturated products were obtained in excellent yields (Table 2, Entry 1–6). No effect of withdrawing and donor groups was observed. The selectivity of Pd_{nano}/MNPs@PU nanoreactors in reduction of cinnamic aldehyde was examined (Table 2, Entry 7); only C=C could be reduced, and 3-phenylpropanal was obtained in a yield of 66%. In addition, the hydrogenation reaction of aromatic alkynes was effective, and fully saturated products were achieved in high yields (Table 2, Entry 8–10). The recyclability of the catalyst was tested in hydrogenation of styrene. The catalyst did not lose its reactivity, and full conversion of styrene to ethylbenzene was obtained in four consecutive cycles. Importantly, no significant change could be observed in the capsule's morphology and size, as confirmed by SEM analysis of the recycled catalyst (Fig. 9). The reaction medium after the separation of the nanoreactors was analyzed using ICP, in which no palladium was detected.

Table 2 Hydrogenation of alkenes and alkynes by Pd_{nano}/MNPs@PU nanoreactors[a]

Entry	Substrate	Product	Yield (%)[b]
1	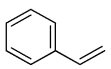	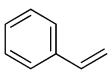	100
2	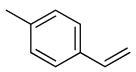	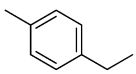	100
3	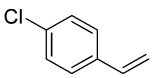	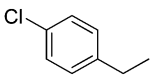	96
4	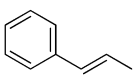	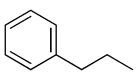	100
5	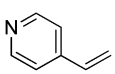	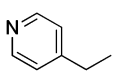	100
6	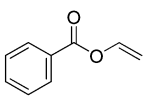	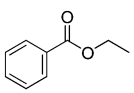	99
7	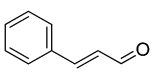	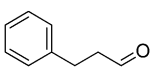	66
8	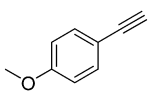	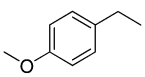	87
9	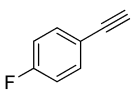	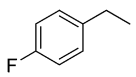	100
10	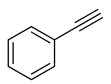	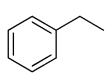	100

[a] 4 mmol of substrate, 2.6×10^{-2} mmol Pd, 2 mL H_2O, 200 psi H_2, room temperature, 6.5 hours. [b] Determined by ^1H NMR and GC.

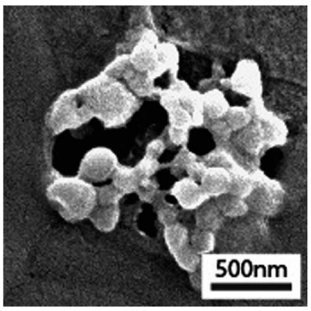

Fig. 9 SEM image of the recycled catalyst Pd_{nano}/MNPs@PU.

Conclusion

The design and immobilization of Pd nanoparticles together with MNPs in polyurea nanocapsules was described. These nanoreactors can be easily separated from the reaction medium by applying an external magnetic field, and act as catalysts in hydrogenation of alkenes and alkynes at room temperature, in aqueous medium. The ability to separate these nanoreactors from the reaction media enables the recyclability of the catalyst.

We anticipate that the method for catalyst immobilization in magnetically separable nanocapsules, developed in this work, can be applied in different fields and may lead to new opportunities in the area of green chemistry.

Experimental section

Materials

Lignosulfonic acid, polymethylene polyphenyl isocyanate and butylated polyvinylpyrrolidone were contributed by FMC Corporation. All other reagents were purchased from either Acros or Sigma-Aldrich, and were used without further purification, with the exception of methyl acrylate, which was purified under reduced pressure.

Instrumentation

NMR measurements were preformed on 400 MHz and 500 MHz Bruker spectrometers. Images were acquired using a high resolution scanning electron microscope (HR SEM), Sirion (FEI Company), using a Schottky type field emission source and a secondary electron (SE) detector. The images were scanned at

5 kV acceleration voltage. Transmission electron microscopy and electron diffraction spectroscopy were performed with a (S) Tecnai F20 G^2 (FEI company), operated at 200 kV. Inductively coupled plasma mass spectrometry measurements were performed on a 7500cx system (Agilent company), using an external standard calibration. Dynamic light scattering measurements were performed using a Nano-zeta sizer (Malvern instruments), model ZEN3600. Gas chromatography (GC) was used to analyze hydrogenation products. GC was performed using an Agilent-GC-7890A with a capillary column (HP-5, 30 meters) and a thermal conductivity detector (TCD). Emulsification was performed using a Kinematica Polytron homogenizer PT-6100, equipped with dispersing aggregates 3030/4EC. Thermogravimetric analysis was performed on a Mettler Toledo TG 50 analyzer. Measurements were carried out at a temperature range that extended from 25–950 °C, at a heating rate of 10 °C min^{-1}, under an air atmosphere. Sonication was performed using a Sonics Vibra Cell, model VCX-130 (130 watt). The average molecular mass of H-PAMAM was determined by matrix assisted laser desorption ionization-time of flight (MALDI-TOF) using a Voyager DE PRO MALDI-TOF mass spectrometer (Applied Biosystems). The mass spectra were acquired using a matrix of α-cyano-4-hydroxycinnamic acid, in the linear positive ion mode by using an accelerating voltage of 25 000 V, a grid voltage of 94%, a guide wire of 0.05%, and an extraction delay time of 340 ms. Surface areas were determined by the N_2 Brunauer–Emmett–Teller method (NOVA-1200e). The pore volume and radius were measured using the BJH model. Powder X-ray diffraction analysis was performed using an X-ray Diffractometer D8 Advance.

Synthesis of hydrophobic magnetite nanoparticles

Magnetite nanoparticles were prepared according to Massart's method.[14] Briefly, 400 mL of H_2O was degassed for 15 min under nitrogen. Then, 11.6 g (42.9 mmol) of $FeCl_3 \cdot 6H_2O$ and 4.3 g (21.6 mmol) of $FeCl_2 \cdot 4H_2O$ were added and heated at 85 °C. 15 mL of concentrated ammonium (28%) was added and the mixture was heated for additional 30 min. After that, 18 mL (57 mmol) of oleic acid was added, resulting in the formation of a black precipitant. The mixture was stirred for an additional 5 min, and then cooled to room temperature. The black precipitant was collected and washed five times with water, five times with acetone, and then dispersed in 50 mL of chloroform.

General procedure for the synthesis of hyperbranched polyamidoamine (H-PAMAM)[15]

Ethylenediamine (18.03 g, 0.3 mol) was dissolved in 28 mL of methanol, and added into a 100 mL single neck flask. Then, methyl acrylate (25.83 g, 0.3 mol) was slowly added, with constant stirring, over a period of 20 minutes. After 48 h of room temperature stirring, methanol was removed under reduced pressure, and the resultant material was heated at 60 °C for 1 h, 100 °C for 2 h, 120 °C for 2 h and 140 °C for 2 h, under vacuum. 34.26 g (95%) of a light yellow viscous dope was obtained. Elementary anal.: C, 51.75; H, 8.56; N, 23.32. ^{1}H NMR ($CDCl_3$): 1.80–2.32 (NH_2–NH), 2.30–2.52 ($COCH_2$), 2.51–3.02 [$COCH_2CH_2NH$, NH $(CH_2)_2NH$, NH $(CH_2)_2NH_2$], 3.20–3.50 (NCH_2), 3.50–4.0 (CH_3O). ^{13}C NMR (D_2O, 125 MHz) δ: 31–59 (CH_2, CH_3), 171–178 (C═O). MALDI-TOF: $m/z = 5798.90$.

General procedure for the synthesis of hyperbranched polyamidoamine (H-PAMAM-C_{15})

Palmitoyl chloride (6 g, 0.0218 mol) was dissolved in 15 mL $CHCl_3$, and added to a solution of H-PAMAM (2 g, 0.083 mol) and triethylamine (6.1 g, 0.044 mol) in 30 mL $CHCl_3$. The reaction mixture was stirred for 24 h at 35 °C under nitrogen. Then, the mixture was cooled to room temperature and washed with 50 mL water three times. The organic layer was collected and dried over anhydrous magnesium sulfate, filtered and concentrated under reduced pressure. The material was poured in 100 mL methanol and the precipitate was collected, washed with methanol and dried under vacuum. 3.5 g (40%) of yellow wax were obtained. Elementary anal.: C, 72.19; H, 12.93; N, 10.97. FTIR (KBr, cm^{-1}) 3311, 2924, 2852, 1644, 1376, 1219, 722, 586. ^{1}H NMR ($CDCl_3$, 500 MHz) δ: 0.87–0.89 (t, 3H, CH_3), 1.24–1.26 (22H, $-CH_2$), 1.52–1.58 (2H, $-CH_2$), 2.29–2.40 (2H, $-NCH_2$), 3.34–3.67 (2H, $-NCH_2$, $-OCH_3$). ^{13}C NMR ($CDCl_3$, 125 MHz) δ: 14.1, 22.68, 23.90, 29.27–29.72, 31.92–31.93, 42.82, 211.

General procedure for preparation of polyurea nanocapsules

The isocyanate monomer (0.7–1.1 g) was dissolved in 8.9 g of $CHCl_3$ and later emulsified with 33.5 g of water, containing a suitable surfactant (2.0 g), by milling at 14 000 rpm for 1 min. Then 5 drops of 1 M HCl were added, the emulsion was sonicated for 17 min and the amine monomer (0.9–1.3 g) was dropped slowly. The resultant mixture was stirred for 16 h at room temperature.

General procedure for preparation of Pd@PU nanoreactors

2.0 g of Reax 88A were dissolved in 33.5 g of water and homogenized for 1 min at 14 000 rpm. Then, 1.1 g of PAPI 27, 0.3 g of H-PAMAM-C_{15}, and 0.15 g of palladium acetate were dissolved in 8.9 g of chloroform and emulsified with the water phase for 1 min. After that, 5 drops of 1 M HCl were added, the emulsion was sonicated for 17 min, and 0.9 g of HMDA (70% in water) was slowly added. Then the solution was stirred for 16 h at room temperature. The next step was to reduce the palladium acetate to Pd nanoparticles, using a glass-lined autoclave. After sealing, the autoclave was purged 3 times with hydrogen and pressurized to 500 psi. The autoclave was stirred at room temperature for 24 h.

General procedure for preparation of Pd/MNPs@PU nanoreactors

The oil phase contains 1.1 g PAPI 27, 1.0 g of MNPs dispersed in 8.9 g of chloroform, 0.3 g H-PAMAM-C_{15} and 0.15 g palladium acetate. Later it was emulsified with the water phase, 2.0 g Reax 88A in 33.5 g water, at 14 000 rpm for 1 min. Then, 5 drops of 1 M HCl were added, the emulsion was sonicated for 17 min and 0.9 g HMDA (70% in water) was slowly added. The solution was stirred for 16 h at room temperature. The formed capsules were

separated using a magnetic field, washed three times each with water, ethanol, and water again. The capsules were dispersed in 50 mL of water, and the palladium acetate was reduced to Pd nanoparticles using a glass-lined autoclave. After sealing, the autoclave was purged 3 times with hydrogen and pressurized to 500 psi. The autoclave was stirred at room temperature for 24 h.

General procedure for the hydrogenation reaction

2.0 g of dispersed nanoreactors containing 0.026 mmol of palladium, 2 mL of water and 4 mmol of the appropriate substrate were placed in a 25 mL glass-lined autoclave. After sealing, the autoclave was purged 3 times with hydrogen and pressurized to 200 psi. The autoclave was stirred at room temperature for 6.5 h, and then the gas was released. The capsules were separated using a magnetic field, washed with water, and used for subsequent cycles. The product was extracted with chloroform and passed through a Celite layer before analysis using NMR and GC.

Notes and references

1 (*a*) *Sustainable Preparation of Metal Nanoparticles: Methods and Applications*, ed. R. Luque and R. S. Varma, The Royal Society of Chemistry, Cambridge, 2013; (*b*) *Nanoparticles and Catalysis*, ed. D. Astruc, Wiley-VCH, Weinheim, 2008; (*c*) *Metal Nanoparticles: Synthesis, Characterization, and Applications*, ed. D. L. Fedlheim and C. A. Foss, Marcel Dekker, New York, 2002.

2 D. Astruc, F. Lu and J. R. Aranzaes, *Angew. Chem., Int. Ed.*, 2005, **44**, 7852.

3 (*a*) V. S. Myers, M. G. Weir, E. V. Carino, D. F. Yancey, S. Pande and R. M. Crooks, *Chem. Sci.*, 2011, **2**, 1632; (*b*) P. L. Duran and G. Rothenberg, *Appl. Organomet. Chem.*, 2008, **22**, 288; (*c*) R. W. J. Scott, O. M. Wilson and R. M. Crooks, *J. Phys. Chem. B*, 2005, **109**, 692; (*d*) R. M. Crooks, M. Zhao, L. Sun, V. Chechik and L. K. Yeung, *Acc. Chem. Res.*, 2001, **34**, 181.

4 (*a*) M. B. Thathagar, J. Beckers and G. Rothenberg, *J. Am. Chem. Soc.*, 2002, **124**, 11858; (*b*) J. S. Bradley, B. Tesche, W. Busser, M. Maase and M. T. Reetz, *J. Am. Chem. Soc.*, 2000, **122**, 4631.

5 (*a*) S. Nath, S. Jana, M. Pradhan and T. Pal, *J. Colloid Interface Sci.*, 2009, **341**, 333; (*b*) J. A. Dahl, B. L. S. Maddux and J. E. Hutchison, *Chem. Rev.*, 2007, **107**, 2228; (*c*) S. U. Son, Y. Jang, K. Y. Yoon, E. Kang and T. Hyeon, *Nano Lett.*, 2004, **4**, 1147.

6 (*a*) Y. Wang, Z. Xiao and L. Wu, *Curr. Org. Chem.*, 2013, **17**, 1325; (*b*) A. Ohtaka, *Chem. Rec.*, 2013, **13**, 274; (*c*) C. T. Campbell and J. R. V. Sellers, *Faraday Discuss.*, 2013, **162**, 9; (*d*) N. J. S. Costa and L. M. Rossi, *Nanoscale*, 2012, **4**, 5826; (*e*) R. J. White, R. Luque, V. L. Budarin, J. H. Clark and D. J. MacQuarrie, *Chem. Soc. Rev.*, 2009, **38**, 481.

7 (*a*) E. Serrano, N. Linares, J. Garcia-Martinez and J. R. Berenguer, *ChemCatChem*, 2013, **5**, 844; (*b*) U. Schubert, *Polym. Int.*, 2009, **58**, 317.

8 (*a*) H. R. Moon, D.-W. Lim and M. P. Suh, *Chem. Soc. Rev.*, 2013, **42**, 1807; (*b*) A. Dhakshinamoorthy and H. Garcia, *Chem. Soc. Rev.*, 2012, **41**, 5262; (*c*) H.-L. Jiang and Q. Xu, *Chem. Commun.*, 2011, **47**, 3351; (*d*) M. Meilikhov, K. Yusenko, D. Esken, S. Turner, T. G. Van and R. A. Fischer, *Eur. J. Inorg. Chem.*, 2010, 3701, DOI: 10.1002/ejic.201000473.

9 (*a*) S. Kobayashi and H. Miyamura, *Chem. Rec.*, 2010, **10**, 271; (*b*) R. Akiyama and S. Kobayashi, *Chem. Rev.*, 2009, **109**, 594.

10 Y. Lan, L. Yang, M. Zhang, W. Zhang and S. Wang, *ACS Appl. Mater. Interfaces*, 2010, **2**, 127.

11 (*a*) H.-J. Xu, X. Wan, Y. Geng and X.-L. Xu, *Curr. Org. Chem.*, 2013, **17**, 1034; (*b*) M. B. Gawande, P. S. Branco and R. S. Varma, *Chem. Soc. Rev.*, 2013, **42**, 3371; (*c*) R. B. N. Baig and R. S. Varma, *Chem. Commun.*, 2013, **49**, 752; (*d*) V. Polshettiwar, R. Luque, A. Fihri, H. Zhu, M. Bouhrara and J.-M. Basset, *Chem. Rev.*, 2011, **111**, 3036; (*e*) Y. Zhu, L. P. Stubbs, F. Ho, R. Liu, C. P. Ship, J. A. Maguire and N. S. Hosmane, *ChemCatChem*, 2010, **2**, 365; (*f*) S. Shylesh, V. Schuenemann and W. R. Thiel, *Angew. Chem., Int. Ed.*, 2010, **49**, 3428; (*g*) C. W. Lim and I. S. Lee, *Nano Today*, 2010, **5**, 412.

12 (*a*) J. Zhou, Z. Dong, H. Yang, Z. Shi, X. Zhou and R. Li, *Appl. Surf. Sci.*, 2013, **279**, 360; (*b*) J. Wang, B. Xu, H. Sun and G. Song, *Tetrahedron Lett.*, 2013, **54**, 238; (*c*) L. M. Rossi, M. A. S. Garcia and L. L. R. Vono, *J. Braz. Chem. Soc.*, 2012, **23**, 1959; (*d*) M. J. Jacinto, F. P. Silva, P. K. Kiyohara, R. Landers and L. M. Rossi, *ChemCatChem*, 2012, **4**, 698; (*e*) B. Liu, W. Zhang, F. Yang, H. Feng and X. Yang, *J. Phys. Chem. C*, 2011, **115**, 15875; (*f*) L. Zhou, C. Gao and W. Xu, *Langmuir*, 2010, **26**, 11217; (*g*) M. J. Jacinto, R. Landers and L. M. Rossi, *Catal. Commun.*, 2009, **10**, 1971; (*h*) R. Abu-Reziq, D. Wang, M. Post and H. Alper, *Adv. Synth. Catal.*, 2007, **349**, 2145.

13 (*a*) Y. Zhang and D. Rochefort, *J. Microencapsulation*, 2012, **29**, 636; (*b*) J. P. Rao and K. E. Geckeler, *Prog. Polym. Sci.*, 2011, **36**, 887.

14 R. Massart, *IEEE Trans. Magn.*, 1981, **MAG-17**, 1247.

15 C.-h. Liu, C. Gao and D.-y. Yan, *Chem. Res. Chin. Univ.*, 2005, **21**, 345.